Laser Light-Scattering Studies of Soluble High Performance Fluorine-Containing Polyimides

SIMON CHI MAN KWAN *and* CHI WU

Department of Chemistry, The Chinese University of Hong Kong
Shatin, N.T., Hong Kong
The Open Laboratory of Bond-Selective Chemistry
Department of Chemical Physics
University of Science and Technology of China
Hefei, Anhui, China

FUMING LI, FRANK W. HARRIS, *and* STEPHEN Z.D. CHENG

Maurice Morton Institute of Polymer Science
Department of Polymer Science.
The University of Akron
Akron, OH, 44325-3909

Two sets of soluble high performance polyimides synthesized from 2,2'-bis(3,4-dicarboxyphenyl)hexafluoropropane dianhydride (6FDA) and 2,2'-(trifluoromethyl)-4,4'-diaminobiphenyl diamine (PFMB), and from 2,2'-bis(trifluoromethyl)-4,4',5,5'-biphenyl-tetracarboxylic dianhydride (HFBPDA) and 2,2'-(trifluoromethyl)-4,4'-di-aminobiphenyl diamine (PFMB) have been investigated by static and dynamic laser light scattering (LLS) in tetrahydrofuran (THF) at 30°C. The calibrations, for 6FDA-PFMB: $<R_g>$ (nm) $= 3.87 \times 10^{-2} <M_w>^{0.568}$, $<R_h>$ (nm) $= 2.38 \times 10^{-2} <M_w>^{0.560}$ and $<D>$ (cm^2/s) $= 2.13 \times 10^{-4} <M_w>^{-0.560}$; for HFBPDA-PFMB: $<R_g>$ (nm) $= 2.24 \times 10^{-2} <M_w>^{0.626}$, $<R_h>$ (nm) $= 1.27 \times 10^{-2} <M_w>^{0.621}$ and $<D>$ (cm^2/s) $= 3.99 \times 10^{-4} <M_w>^{-0.621}$, have been established, where $<M_w>$, $<R_g>$, $<R_h>$ and $<D>$ are the weight-average molar mass, the root mean square z-average radius of gyration, the z-average hydrodynamic radius and the z-average translational diffusion coefficient, respectively. A combination of $<M_w>$ and the translational diffusion coefficient distribution $G(D)$ leads to the calibrations of D (cm^2/s) $= 2.41 \times 10^{-4} M^{-0.564}$ and D (cm^2/s) $= 6.16 \times 10^{-4} M^{-0.656}$ for 6FDA-PFMB and HFBPDA-PFMB, respectively, where D and M correspond to monodisperse species. With these calibrations, we can convert a translational diffusion coefficient distribution $G(D)$ into a corresponding molar mass distribution $f_w(M)$. On the basis of the Kratky-Porod wormlike chain model, the persistence lengths (q) were found to be ~ 3.3 nm and ~ 4.5 nm, respectively, for 6FDA-PFMB and HFBPDA-PFMB, which indicates that both polyimide chains have an extended conformation. In addition, $<R_g>/<R_h> \sim (1.7-1.9)$ shows that they are in coil conformation. Therefore, we conclude that both polyimides have an extended coil conformation.

INTRODUCTION

Aromatic polyimides have been being widely used in making films, coatings, fibers, and adhesives because of their high thermal stability and excellent mechanical properties (1, 2). Recently, polyimides with low dielectric constant, low water adsorption, and low thermal expansion have been applied to electronic devices (3). Therefore, investigating microscopic parameters of polyimide chains is very important to the development of more advanced polyimide related materials.

However, it is hard to dissolve polyimides in common organic solvents because of their chain stiffness, which hinders the study of their solution properties. In the past, the molecular parameters of insoluble polyimides had to be estimated from their precursors, i.e., from polyamic acid formed in the first stage of the reaction between diamines and anhydrides. The estimation involves problems, such as the polyelectrolytes effect in the precursor solution and the structure discrepancy between the precursor and final polymer (4, 5).

Recently, soluble high performance polyimides have been developed (6, 7). The dissolution is achieved by introducing some side groups, such as –CH$_3$ and –CF$_3$, in the polymer chain to twist the aromatic imide rings and the phenyl groups in order to decrease the

chain-to-chain interaction. In addition, some joints, such as –O– and –CH$_2$–, are used to separate the aromatic imide rings and the phenyl rings so as to increase the chain flexibility. Recent investigations have shown that introducing the fluorinated groups, the refractive index, water adsorption and dielectric constant of polyimides are significantly reduced [8–10], which is important to the development of electronic devices.

In this study, two kinds of polyimides, 6FDA-PFMB and HFBPDA-PFMB, were made individually by a one-step polycondensation of 2,2'-bis(3,4-dicarboxy-phenyl)hexafluoro-propane dianhydride (6FDA) and 2,2'-(trifluoromethyl)-4,4'-diaminobiphenyl diamine (PFMB), and of 2,2'-bis(trifluoromethyl)-4,4',5,5'-biphenyltetracarboxylic dianhydride (HFBPDA) and 2,2'-(trifluoromethyl)-4,4'-diaminobiphenyl diamine (PFMB), respectively [11, 12]. In comparison with the conventional two-step reaction, higher molar mass polyimides were obtained. The structure of 6FDA-PFMB and HFBPDA-PFMB are as follows:
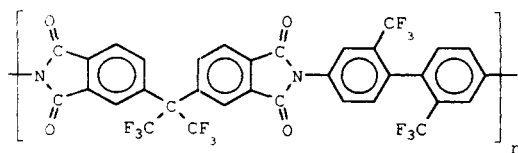
6FDA-PFMB
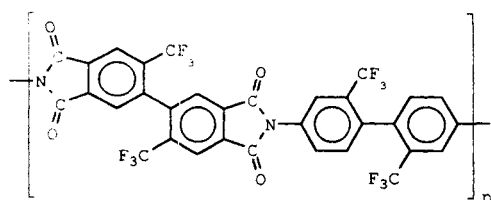
HFBPDA-PFMB

The backbone of these polyimides contain four trifluoromethyl groups, which enhances their solubility in common organic solvents, such as tetrahydrofuran (THF) and methyl ethyl ketone (MEK).

EXPERIMENTAL

Sample Preparation. The synthesis of 6FDA-PFMB and HFBPDA-PFMB has been described [11,12]. 6FDA and PFMB or HFBPDA and PFMB were dissolved in organic solvents such as *m*-cresol and polycondensed under reflux. Five 6FDA-PFMB and seven HFBPDA-PFMB fractions were obtained using a Waters Fraction Collector in conjunction with a Waters 150 CV chromatography system consisted of a series of four Waters Ultrastyragel columns in the order of 10^5, 10^4, 10^3, and 10^2 nm, wherein analytical reagent grade THF was used as the mobile phase and the flow rate was 1.0 mL/min. The collected fractions were transferred into flasks to evaporate the solvent and were dried in vacuum for 24 hours at 125°C prior to the experiments. According to the fractionation order, they were termed as, for 6FDA-PFMB: 6FDA-1,

6FDA-2, 6FDA-3, 6FDA-4 and 6FDA-5; for HFBPDA-PFMB: HF-1, HF-2, HF-3, HF-4, HF-5, HF-6 and HF-7 hereafter. Analytical reagent grade THF as solvent was dried by sodium and then distilled under nitrogen before use. All polymer solutions were filtered at room temperature using 0.5-μm PTFE membrane.

Laser Light Scattering (LLS). A modified commercial light-scattering spectrometer (ALV/SP-125) equipped with an ALV-5000 multi-τ digital time correlator and a solid state laser (ADLAS DPY 425II, output power ≈ 400 mW at λ_o = 532 nm) as the light source was used. The primary beam is vertically polarized with respect to the scattering plane. In static LLS, the instrument was calibrated with toluene to make sure that the scattering intensity from toluene has no angular dependence in the range of 15°–150°. The details of the LLS instrumentation and theory can be found elsewhere [13, 14]. All LLS measurements were carried out at 30.0 ± 0.1 °C. In static LLS, the angular dependence of the excess absolute time-averaged scattered intensity, known as the excess Rayleigh ratio, $R_{vv}(q)$, was measured. For a dilute polymer solution measured at a low scattering angle, $R_{vv}(q)$ can be related to the weight-average molar mass, $<M_w>$, the second virial coefficient, A_2, and root mean square z-average radius of gyration, $<R_g^2>_z^{1/2}$ (or simply written as $<R_g>$), as [15]

$$\frac{KC}{R_{vv}(q)} \approx \frac{1}{<M_w>}\left(1 + \frac{1}{3}<R_g^2>_z q^2\right) + 2A_2C \quad (1)$$

where $K = 4\pi^2 n^2 (dn/dC)^2/(N_A\lambda_0^4)$ and $q = (4\pi n/\lambda_0)\sin(\theta/2)$ with N_A, dn/dC, n and λ_0 being Avogadro number, the specific refractive index increment, the solvent refractive index and the wavelength of light in vacuum, respectively. Measuring $R_{vv}(q)$ at a set of C and q, we are able to determine $<M_w>$, $<R_g>$, and A_2 from a Zimm plot which incorporates the extrapolations of $q \to 0$ and $C \to 0$ on a single grid. The dn/dC was measured using a recently developed novel refractometer [16].

In dynamic LLS, a precise intensity-intensity time correlation function $G^{(2)}(t, q)$ in the self-beating mode was measured and $G^{(2)}(t, q)$ is related to the normalized first-order electric field time correlation function $g^{(1)}(t, q)$ as [14]

$$G^{(2)}(t, q) = <I(t, q)I(0, q)> = A[1 + \beta|g^{(1)}(t, q)|^2] \quad (2)$$

where A is a measured base line; β, a parameter depending on the coherence of the detection; and t, the delay time. It should be stated that in this study A is not an adjustable parameter. Instead, we insisted on the agreement between A and the calculated baseline within 0.1 % in all dynamic LLS experiments. This requires a very careful solution preparation (i.e., dust free).

RESULTS AND DISCUSSION

The refractive index increment (Δn) was found to depend linearly on concentration (C) for 6FDA-PFMB

Simon Chi Man Kwan, Chi Wu, Fuming Li, Frank W. Harris, and Stephen Z. D. Cheng

and HFBPDA-PFMB in THF at 30°C. A least-square fitting of the lines leads to a specific refractive index increment (dn/dC) = 0.182 ± 0.002 mL/g and 0.148 ± 0.002 mL/g for 6FDA-PFMB and HFBPDA-PFMB, respectively, at T = 30.0°C and λ_0 = 532 nm. Equation 1 shows that both $<M_w>$ and A_2 depend on the square of dn/dC, so that the accurate dn/dC value has ensured a good characterization of $<M_w>$ and A_2.

Figure 1 shows a Zimm plot for HF-5 in THF at 30°C. From each Zimm plot, we were able to determine the values of $<M_w>$, $<R_g>$ and A_2 respectively from the extrapolations of $[KC/R_{vv}(q)]_{c\to0,\theta\to0}$, $[KC/R_{vv}(q)]_{c\to0}$ versus q^2 and $[KC/R_{vv}(q)]_{\theta\to0}$ versus C. The static LLS results are summarized in Table 1. The positive A_2 values indicate that THF is a good solvent for the both polyimides at 30°C. The 6FDA-1, 6FDA-2, HF-1, HF-2 and HF-3 chains are so short that $R_{vv}(\theta)$ practically shows no angular dependence and their $<R_g>$ values cannot be accurately determined. The calibrations, for 6FDA-PFMB: $<R_g>$ (nm) = 3.87 × $10^{-2}<M_w>^{0.568}$, and for HFBPDA-PFMB: $<R_g>$ (nm) = 2.24 × $10^{-2}<M_w>^{0.626}$ were established where the $<R_g>$ values of 6FDA-1, 6FDA-2, HF-1, HF-2 and HF-3 are estimated from their corresponding $<R_h>$ values and their corresponding average value of the ratio $<R_g>/<R_h>$.

Figure 2 shows a measured intensity-intensity time correlation function for 6FDA-3 in THF at θ = 30° and T = 30°C. It is known that for a polydisperse sample $g^{(1)}(t, q)$ is related to the line-width distribution $G(\Gamma)$ by (14)

$$g^{(1)}(t, q) = <E(t, q)E^*(0, q)> = \int_0^\infty G(\Gamma)e^{-\Gamma t}d\Gamma \quad (3)$$

The Laplace inversion program CONTIN equipped with the correlator was used in this work to convert $G^{(2)}(t, q)$ to $G(\Gamma)$ on the basis of Eqs 2 and 3. The left insert in Fig. 2 shows a typical $G(\Gamma)$. In the case of $<R_g^2>_z q^2<<1$, the line width Γ usually depends on both C and q as (17, 18),

$$\Gamma/q^2 = D(1 + k_d C)(1 + f<R_g^2>_z q^2) \quad (4)$$

where D is the translational diffusion coefficient at $C \to 0$ and $q \to 0$; k_d, the diffusion second virial coefficient; and f, a dimensionless parameter depending on the chain structure, polydispersity, and solvent quality. k_d reflects both the thermodynamic and hydrodynamic interactions, i.e., $k_D = 2A_2<M_w> - C_D N_A R_h^3/<M_w>$, where C_D is a constant and R_h is the hydrodynamic radius. The values of D, f, and k_d respectively obtained from the plots $(\Gamma/q^2)_{c\to0,\theta\to0}$, $(\Gamma/q^2)_{c\to0}$ versus q^2 and $(\Gamma/q^2)_{\theta\to0}$ versus C are also listed in Table 1. No angular dependence of (Γ/q^2) is observed in some low molecular weight fractions, implying that the values of $f<R_g^2>_z q^2$ are very small. This is understandable because the size of polymers is so small that the contribution of internal motions to the relaxation is insignificant (13, 19). In a good solvent $(A_2 > 0)$, Γ/q^2 is less dependent on C than $R_{vv}(\theta)$ because of a partial cancellation of the thermodynamic term $2A_2<M_w>$ by the hydrodynamic interaction $(C_D N_A R_h^3/<M_w>)$. In the case of $C \sim 10^{-4}$ and
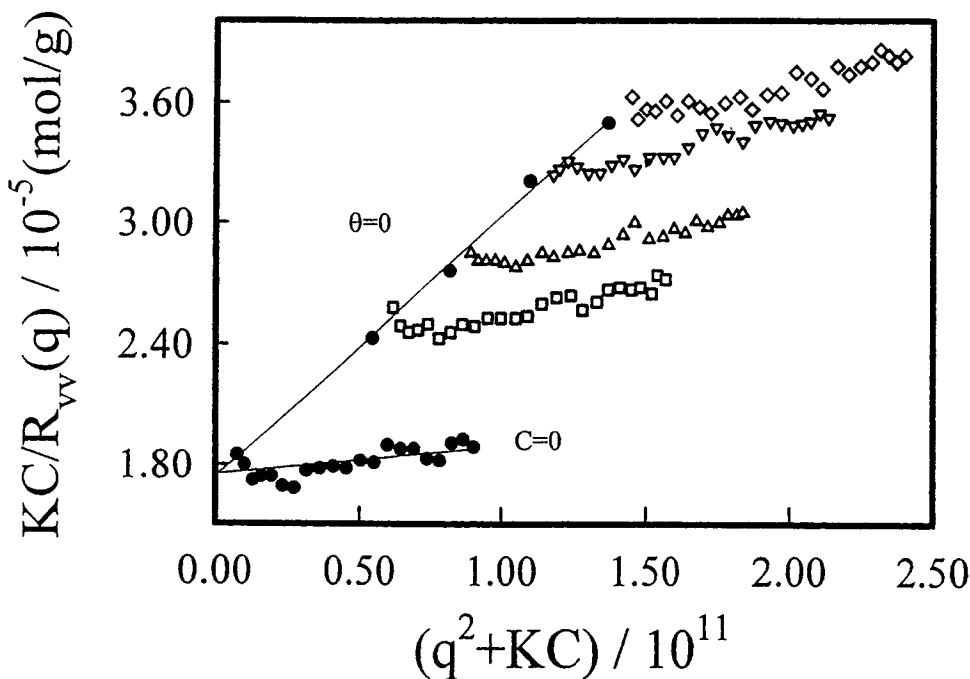
Fig. 1. A Zimm-plot of HF-5 in THF at T = 30°C, where the concentration of the polymer solution ranges from 0.4 × 10^{-3} g/ml to 2 × 10^{-3} g/mL.

$\theta < 30°$, $(1 + k_dC)(1 + f<R_g^2>_z q^2) \sim 1$, so that $\Gamma/q^2 = D$ and $G(\Gamma)$ can be directly transformed into a translational diffusion coefficient distribution $G(D)$ or a hydrodynamic radius distribution $f(R_h)$ using the Stokes-Einstein equation: $D \equiv k_B T/(6\pi\eta R_h)$, where k_B, T, and η, are the Boltzmann constant, the absolute temperature, and solvent viscosity, respectively.

The right insert in Fig. 2 shows the corresponding translational diffusion coefficient distributions $G(D)$ of the polyimides in THF at $T = 30°C$. From each $G(D)$, we were able to calculate a z-average translational diffusion coefficient $<D> = \int_0^\infty G(D)D\ dD$, where $G(D)$ is z-average, and an z-average hydrodynamic radius $<R_h>$ after replacing D in the Stokes-Einstein equation with $<D>$. The values of $<D>$, $<R_h>$, and $<R_g>/<R_h>$ of all fractions of both polyimides are also summarized in Table 1. The ratio of $<R_g>/<R_h>$ are in the range of $\sim 1.7 - 1.9$, higher than ~ 1.5 predicted for monodisperse random coil chains (17, 20, 21), but close to ~ 1.84 predicted for random coil chains with a polydispersity index $(<M_w>/<M_n>)$ of ~ 2.

Figure 3 shows $\log(<D>)$ is a linear function of $\log(<M_w>)$ of 6FDA-PFMB and HFBPDA-PFMB respectively. The solid lines represent a least-square fitting of $<D> = <k_D> M_w^{-<\alpha_D>}$ with, for 6FDA-PFMB: $<k_D> = 2.13 \times 10^{-4}$ and $<\alpha_D> = 0.560$, and for HFBPDA-PFMB: $<k_D> = 3.99 \times 10^{-4}$ and $<\alpha_D> = 0.621$, where $<\ >$ means that the values of $<k_D>$ and $<\alpha_D>$ were obtained from $<D>$ and $<M_w>$ rather than from D and M for monodisperse species. The value of $<\alpha_D>$ of HFBPDA-PFMB is greater than that of 6FDA-PFMB which means that the HFBPDA-PFMB

chains in THF at $T = 30°C$ has a more extended conformation.

Knowing k_D and α_D, we can transfer each $G(D)$ into a molar mass distribution using (17, 20, 21)

$$f_w(M) \propto \frac{G(D)D}{M^2} \propto G(D)D^{1 + 2/\alpha_D} \tag{5}$$

According to the definition of $<M_w>$ $[= \int_0^\infty f_w(M)M dM / \int_0^\infty f_w(M)dM]$ and Eq 5, we have

$$(<M_w>)_{calcd} = \frac{k_D^{1/\alpha_D} \int_0^\infty G(D)dD}{\int_0^\infty G(D)D^{1/\alpha_D}dD} \tag{6}$$

If approximating k_D and α_D with $<k_D>$ and $<\alpha_D>$, we found that the calculated values of $<M_w>$ of both polyimides fractions are much smaller than the values of $<M_w>$ directly measured in static LLS. This disagreement is understandable because $<k_D> \neq k_D$ and $<\alpha_D> \neq \alpha_D$ for the moderately distributed 6FDA-PFMB and HFBPDA-PFMB fractions.

Our previous studies have shown a method of combining static and dynamic LLS results to obtain k_D and α_D from the measured values of $<M_w>$ and $G(D)$ (17,21-24). Using this combination method, we found that, for 6FDA-PFMB: $k_D = 2.41 \times 10^{-4}$ and $\alpha_D = 0.564$, and for HFBPDA-PFMB: $k_D = 6.16 \times 10^{-4}$ and $\alpha_D = 0.656$. These pairs of k_D and α_D define the calibrations between D and M for monodisperse 6FDA-PFMB and HFBPDA-PFMB in THF at $T = 30°C$, shown
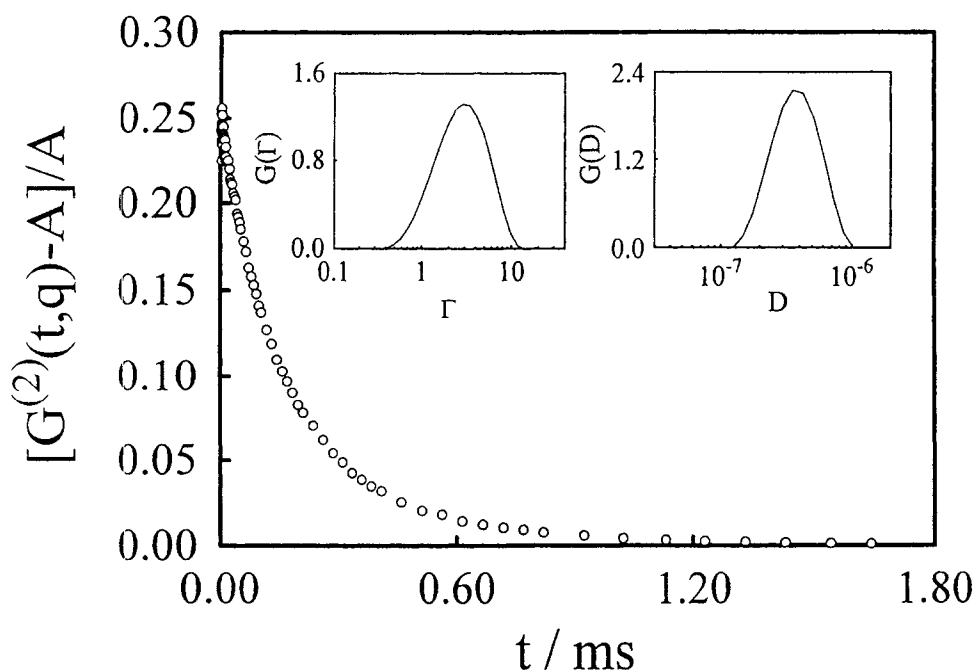
Fig. 2. A measured intensity-intensity time correlation function for 6FDA-3 in THF at $\theta = 30°$ and $T = 30°C$. The left insert shows a corresponding line-width distribution $G(\Gamma)$ calculated from $G^{(2)}(t,q)$. The right insert shows a corresponding translational diffusion coefficient distribution $G(D)$ calculated from $G(\Gamma)$.

Simon Chi Man Kwan, Chi Wu, Fuming Li, Frank W. Harris, and Stephen Z. D. Cheng
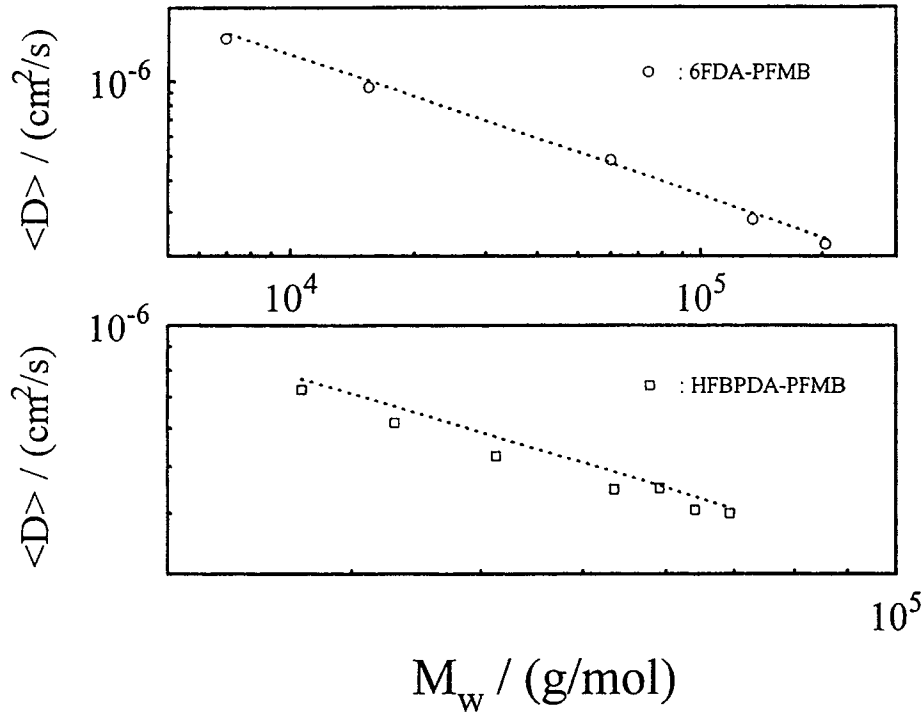
Fig. 3. Two double logarithmic plots of $<D>$ vs $<M_w>$. For 6FDA-PFMB, the solid line represents the least-square fitting of $<D>$ $(cm^2/s) = 2.13 \times 10^{-4}<M_w>^{-0.560}$; and the dotted line, D $(cm^2/s) = 2.41 \times 10^{-4}M^{-0.564}$ for monodisperse species. For HFBPDA-PFMB, the solid line represents the least-square fitting of $<D>$ $(cm^2/s) = 3.99 \times 10^{-4}<M_w>^{-0.621}$; and the dotted line, D $(cm^2/s) = 6.16 \times 10^{-4}M^{-0.656}$ for monodisperse species.
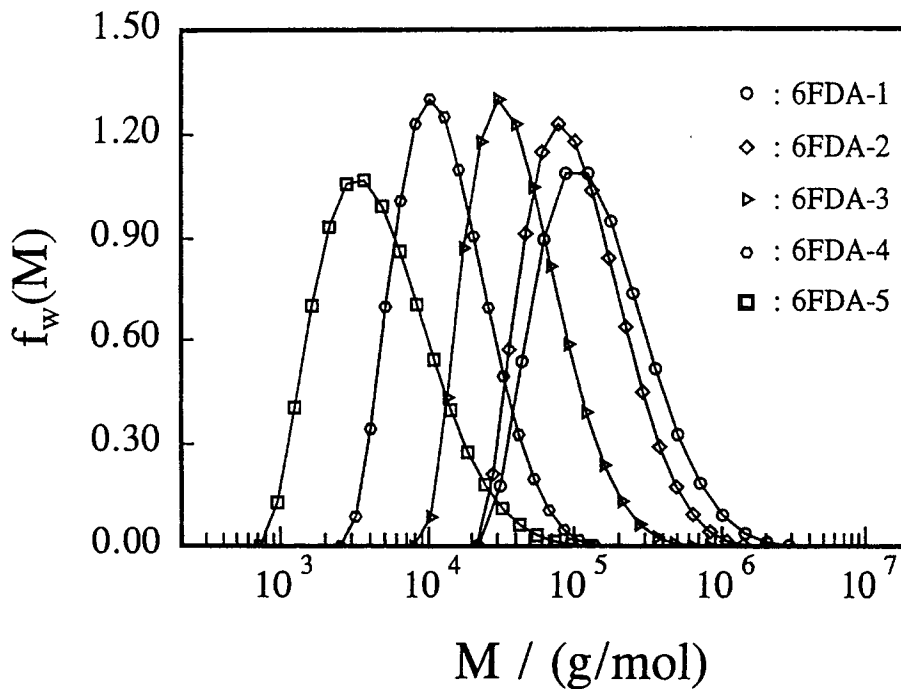
Fig. 4. Molar mass distributions of five 6FDA-PFMB fractions.
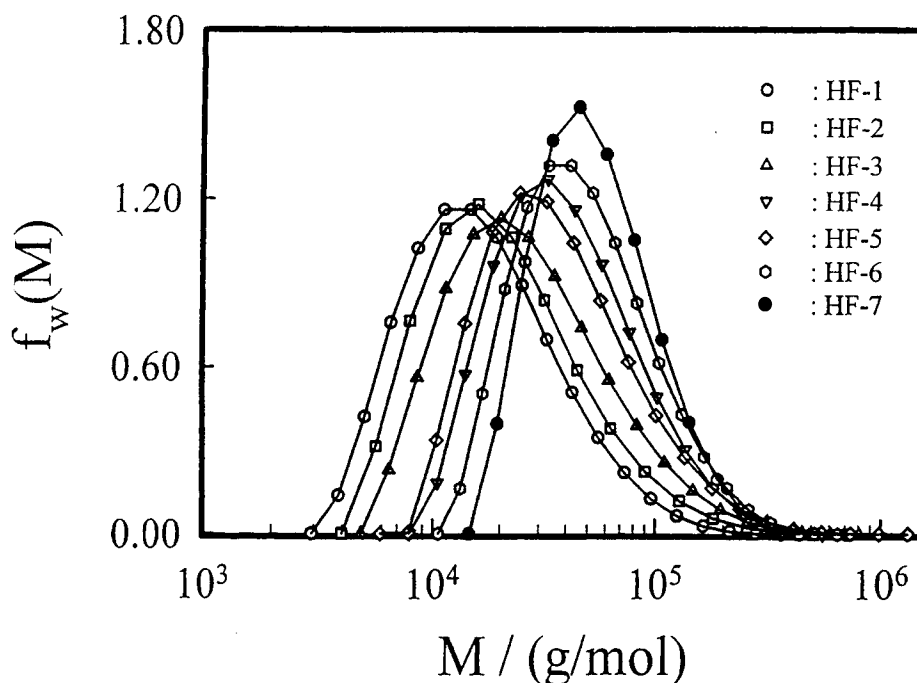
Fig. 5. Molar mass distributions of seven HFBPDA-PFMB fractions.

Table 1. Summary of Static and Dynamic Laser Light-Scattering Results of Fractions of both Polyimides.

Sample	10^{-4} $<M_w>$ (g/mol)	$<R_g>$ (nm)	$10^4 A_2$ (mol·cm^3/g^2)	$10^8 <D>$ (cm^2/s)	k_d mL/g	f	$<R_h>$ (nm)	$<R_g>/<R_h>$	$10^{-4}(<M_w>)_{calcd}$ (g/mol)	M_z/M_w	M_w/M_n
6FDA-1	0.69	—	53.4	149	~0	~0	3.38	—	0.68	2.4	2.0
6FDA-2	1.54	—	23.0	94.8	13	~0	5.35	—	1.64	1.7	1.6
6FDA-3	5.99	17.4	28.2	48.2	27	~0	10.5	1.66	5.37	1.8	1.6
6FDA-4	13.4	32.4	11.2	28.1	41	~1	18.0	1.80	13.9	1.9	1.7
6FDA-5	20.3	41.9	10.3	22.4	75	~1	22.6	1.85	20.0	2.2	1.9
HF-1	2.69	—	22.1	72.6	30	~0	6.99	—	2.63	1.9	1.7
HF-2	3.30	—	14.2	61.7	29	~0	8.23	—	3.33	2.1	1.8
HF-3	4.14	—	27.6	52.6	31	~0	9.63	—	4.24	2.0	1.8
HF-4	5.35	20.7	13.9	44.8	-26	~0	11.3	1.83	5.60	1.7	1.6
HF-5	5.92	20.8	23.9	45.0	25	~0	11.3	1.84	5.44	1.9	1.7
HF-6	6.41	23.3	20.4	40.7	80	~0	12.4	1.88	6.53	1.6	1.5
HF-7	6.93	24.0	17.5	40.0	52	~0	12.7	1.89	6.84	1.4	1.4

The relative errors: $<M_w>$, ± 5%; $<R_g>$, ± 10-15%; A_2, ± 15%; $<D>$, ± 3%.

in *Fig. 3* by the dotted line. With this pair of k_D and α_D, we converted each $G(D)$ to a corresponding $f_w(M)$.

Figures 4 and *5* show molar mass distributions $f_w(M)$ of five 6FDA-PFMB and seven HFBPDA-PFMB fractions. From each $f_w(M)$, we calculated a corresponding weight-average molar mass $(<M_w>)_{calcd}$ and polydispersity index $<M_w>/<M_n>$ and $<M_z>/<M_w>$, which are also listed in *Table 1*. The calculated values of $(<M_w>)_{calcd}$ agree well with the measured values of $<M_w>$ from static LLS. The values of $<M_w>/<M_n>$ ≤ 2 are expected since both polyimides were made by polycondensation followed by fractionation. For 6FDA-1, the measured $G(D)$ may contain some experimental noise which make the width of $G(D)$ larger, hence the abnormal larger PI value is obtained. We can estimate the persistence length (q) on the basis of Kratky-Porod

wormlike chain model (25),

$$\langle R_g^2 \rangle = q^2 \left\{ \frac{1}{3}\left(\frac{L}{q}\right) - 1 + \left(\frac{2q}{L}\right) - \left(\frac{2q^2}{L^2}\right)\left[1 - exp\left(-\frac{L}{q}\right)\right] \right\}$$

(7)

where L $(= n\ell_u)$ is the contour length with ℓ_u being the projected length of the monomer unit and n $(= <M_w>/M_o)$ being the average number of the monomers unit of polymer chain. In this case, ℓ_u and M_o are, for 6FDA-PFMB: ~ 2.18 nm and 728 g/mol respectively, and for HFBPDA-PFMB: ~ 2.08 nm and 714 g/mol respectively. Strictly speaking, we should use $n = (<M_z>/<M_w>)(<M_w>/<M_o>)$ since $<R_g>$ measured in static LLS is a z-averaged parameter. The values of q estimated from the values of $<R_g^2>$ and

Simon Chi Man Kwan, Chi Wu, Fuming Li, Frank W. Harris, and Stephen Z. D. Cheng

$<M_w>$ of 6FDA-PFMB and HFBPDA-PFMB are $\sim$ 3.3 nm and $\sim$ 4.5 nm respectively. In comparison with the value of $q \sim 1$ nm for typical flexible polymers, such as polystyrene and polymethyl methacrylate in good solvent, both polyimides chains have a more extended conformation in THF at 30°C. The extended conformation can be attributed to the rigid segments in the backbone. It is also possible that the extended conformation is related to the excluded volume effect (26). *Equation 7* shows that when $L/q \to 0$, $<R_g^2> \to L^2/12$ and the polymer becomes a rigid rod; on the other hand, when $L/q >> 1$, the polymer chain becomes a coil and $<R_g^2> = <h^2>/6$, where $<h^2>$ (= $2qL$) is the mean square end-to-end distance of the polymer chain. Assuming both polyimides chains have a coil conformation, the estimate of q from $<R_g^2>$ through $<h^2>$ are $\sim$ 3.3 nm and $\sim$ 4.5 nm for 6FDA-PFMB and HFBPDA-PFMB, respectively, which are very close to the results calculated on the basis of *Eq 7*, implying that the both polyimides chains have an extended coil conformation.

The chain flexibility can be attributed to the rotating joints, such as -O-, -S-, -CH_2-, and a single bond between the rigid-rod segments (26, 27). Since the chain flexibility contributed by -CH_2- joint is normally greater than that by a single bond, the coil conformation of the HFBPDA-PFMB chain is more extended than that of 6FDA-PFMB, which is supported by the higher persistence length and the greater values of the exponents of the calibrations of HFBDPA-PFMB.

The chain dimensions of 6FDA-PFMB and HFBPDA-PFMB were compared with polystyrene in a good solvent. The comparisons were calculated by the calibrations $<R_g> \sim N$ and $<R_h> \sim N$ of the polymers where N is the average number of C-C bonds of the polymer chain. The average number of C-C bonds per monomer unit are 2, 14.2 (2.18 nm $\div$ 0.154 nm) and 13.5 (2.08 nm $\div$ 0.154 nm) for polystyrene, 6FDA-PFMB and HFBPDA-PFMB, respectively where the average C-C bond length is 0.154 nm. The calibrations are, for polystyrene (28), R_g (nm) = $1.13 \times 10^{-1}N^{0.620}$ and R_h (nm) = $9.77 \times 10^{-2}N^{0.577}$; for 6FDA-PFMB: R_g (nm) = $3.62 \times 10^{-1}N^{0.568}$ and R_h (nm) = $2.17 \times 10^{-1}N^{0.560}$; for the HFBPDA-PFMB: R_g (nm) = $2.69 \times 10^{-1}N^{0.626}$ and R_h (nm) = $1.51 \times 10^{-1}N^{0.620}$. The values of R_g and R_h of the two polyimides are generally two times higher than that of polystyrene at the same value of N (when $N >> 1$). This indicates that the coil conformation of both polyimides is more expanded than that of polystyrene. This expansion is attributed to the excluded volume effect and the chain stiffness.

CONCLUSIONS

A combination of static and dynamic laser light scattering (LLS) studies of 6FDA-PFMB and HFBPDA-PFMB in THF at 30°C shows that:

i) The persistence lengths (q) of 6FDA-PFMB and HFBPDA-PFMB are $\sim$ 3.3 nm and $\sim$ 4.5 nm, re-

spectively, and the ratios of $<R_g>/<R_h>$ are in the range of 1.7–1.9;

ii) $<R_g>$, $<R_h>$ and D are scaled to the molar mass as for 6FDA-PFMB: $<R_g>$ (nm) = $3.87 \times 10^{-2}<M_w>^{0.568}$, $<R_h>$ (nm) = $2.38 \times 10^{-2}<M_w>^{0.560}$ and D (cm^2/s) = $2.41 \times 10^{-4}M^{-0.564}$, for HFBPDA-PFMB: $<R_g>$ (nm) = $2.24 \times 10^{-2}<M_w>^{0.626}$, $<R_h>$ (nm) = $1.27 \times 10^{-2}<M_w>^{0.621}$ and D (cm^2/sec) = $6.16 \times 10^{-4} \times M^{-0.656}$, respectively;

iii) both 6FDA-PFMB and HFBPDA-PFMB chains have an expanded coil conformation; and iv) It was found that the HFBPDA-PFMB chains are more extended than the 6FDA-PFMB chains because HFBPDA-PFMB chains contain a less flexible single bond joint instead of the -CH_2- joint in 6FDA-PFMB chains.

v) Using the calibration between D and M, we have successfully converted each translational diffusion coefficient distribution into a corresponding molar mass distribution, which demonstrates that the molar mass distribution of 6FDA-PFMB and HFBPDA-PFMB can be easily characterized by LLS using only one dilute solution measured at one scattering angle.

NOMENCLATURE

6FDA-PFMB = Polyimide synthesized from 2,2'-bis(3,4-dicarboxyphenyl)hexafluoropropane dianhydride (6FDA) and 2,2'-(trifluoromethyl)-4,4'diaminobiphenyl diamine (PFMB).

A = The measured baseline.

A_2 = Second virial coefficient.

C = Concentration of polymer solutions.

D = Translational diffusion coefficient.

$<D>$ = z-average translational diffusion coefficient.

dn/dC = The specific refractive index increment.

$E(t,q)$ = Scattered electric field.

$f_w(M)$ = Molar mass distribution.

f = A dimensionless number depending the angular dependence of $<D>$.

$G(\Gamma)$ = Normalized linewidth distribution.

$G^{(2)}(t,q)$ = Intensity-intensity time correlation function.

$g^{(1)}(t,q)$ = Normalized first-order electric field time correlation function.

$G(D)$ = Translational diffusion coefficient distribution.

$<h^2>$ = Mean square end-to-end distance.

HFBPDA-PFMB = Polyimide synthesized from 2,2'-bis(trifluoro-methyl)-4,4',5,5'-biphenyltetracarboxylic dianhydride (HFBPDA) and 2,2'-(trifluoromethyl)-4,4'-diaminobiphenyl diamine (PFMB).

$I(t,q)$ = Scattered intensity.

k_d = The diffusion second virial coefficient.

k_B = The Boltzmann constant.

L = Contour length.

ℓ_u = Projection length of monomer unit.

LLS = Laser light scattering.

$<M_w>$ = Weight-average molar mass.

MEK = Methyl ethyl ketone.

M = Molar mass for monodisperse compounds.

M_o = Monomer mass.

$(<M_w>)_{calcd}$ = The calculated weight-average molar mass.

N_A = Avogadro's number.

n = Solvent refractive index.

N = Number of carbon-carbon bonds in the polymer chain.

$<R_h>$ = z-average hydrodynamic radius.

$<R_g>$ = Root mean square z-average radius of gyration.

$R_{vv}(q)$ = The excess Rayleigh ratio.

q = Persistence length.

q = Scattering vector.

THF = Tetrahydrofuran.

T = Absolute temperature.

λ_o = Wavelength of light in vacuum.

Γ = Linewidth.

β = The parameter depending on the coherence of the detection.

Δn = Refractive index increment.

η = Solvent viscosity.

REFERENCES

1. N. A. Adrova and N. Aleksandrovna, *Polyimides: A New Class of Heat-Resistant Polymers*, Jerusalem (1969).
2. D. Wilson, H. D. Stengenberger, and P. M. Hergenrother, *Polyimides*, Chapman and Hall, New York (1990).
3. A. J. Kirby, *Polyimides: Materials, Processing and Application*, Rapra Technology, Ltd., Shrewsbury, Shropshire, United Kingdom (1992).
4. P. M. Cotts, in *Polyimides: Synthesis, Characterization, and Applications*, Plenum Press, New York (1984).
5. S. Kim, P. M. Cotts, and W. Volksen, *J. Polym. Sci. Polym. Phys.*, **30**, 177 (1992).
6. T. Matsuura, Y. Hasuda, S. Nishi, and N. Yamada, *Macromolecules*, **24**, 5001 (1991).
7. S. Z. D. Cheng, Z. Q. Wu, M. Eashoo, S. L. C. Hsu, and F. W. Harris, *Polymer*, **32**, 1803 (1991).
8. A. E. Feiring, B. C. Auman, and E. R. Wonchoba, *Macromolecules*, **26**, 2779 (1993).
9. T. Matsuura, M. Ishizawa, Y. Hasuda, and S. Nishi, *Macromolecules*, **25**, 3540 (1992).
10. G. Hougham, G. Tesoro, and J. Shaw, *Macromolecules*, **27**, 3642 (1994).
11. S. L.-C. Hsu, PhD dissertation, Department of Polymer Science, The University of Akron, Akron, Ohio (1991).
12. S. Lin, PhD dissertation, Department of Polymer Science, The University of Akron, Akron, Ohio (1994).
13. R. Pecora and J. Berne, *Dynamic Light Scattering*, Plenum Press, New York (1976).
14. B. Chu, *Laser Light Scattering*, 2nd Ed., Academic Press, New York (1991).
15. B. H. Zimm, *J. Chem. Phys.*, **16**, 1099 (1948).
16. C. Wu, and K. Q. Xia, *Rev. Sci. Instrum.*, **65**, 587 (1994).
17. W. H. Stockmayer and M. Schmidt, *Pure Appl. Chem.*, **54**, 407 (1982).
18. W. H. Stockmayer and M. Schmidt, *Macromolecules*, **17**, 509 (1984).
19. W. Brown and T. Nicolai, in *Dynamic Light Scattering: The Method and Some Application*, W. Brown, ed., Oxford University Press Inc., New York (1993).
20. W. Burchard, M. Schmidt, and W. H. Stockmayer, *Macromolecules*, **13**, 1265 (1980).
21. G. Vancso *et al.*, *Macromolecules*, **21**, 415 (1988).
22. C. Wu, *J. Polym. Sci. Polym. Phys.*, **32**, 803 (1994).
23. C. Wu, *Colloid Polym. Sci.*, **271**, 947 (1993).
24. C. Wu, J. Zuo, and B. Chu, *Macromolecules*, **22**, 633 (1989).
25. H. Benoit, and P. Doty, *J. Phys. Chem.*, **57**, 958 (1953).
26. S. Ya. Magarik, in *Polyamic Acids and Polyimides: Synthesis, Transformations, and Structure*, M. I. Bessonov and V. A. Zubkov, eds., CRC Press (1993).
27. S.-S. A. Pavlova, G. I. Timofeeva, and I. A. Ronova, *J. Polym. Sci. Polym. Phys. Ed.*, **18**, 1175 (1980).
28. B. Appelt and G. Meyerhoff, *Macromolecules*, **13**, 657 (1980).